

## Catalytic pyrolysis of corn straw for deoxygenation of bio-oil with different types of catalysts

Wenkai Zhang<sup>\*\*\*</sup>, Ze Wang<sup>\*\*\*,†</sup>, Tengze Ge<sup>\*\*\*</sup>, Cuiguang Yang<sup>\*\*\*\*</sup>,  
Wenli Song<sup>\*\*\*</sup>, Songgeng Li<sup>\*\*\*</sup>, and Rui Ma<sup>\*</sup>

<sup>\*</sup>State Key Laboratory of Multi-Phase Complex Systems, Institute of Process Engineering,  
Chinese Academy of Sciences, 100190, China

<sup>\*\*</sup>Sino-Danish College, University of Chinese Academy of Sciences/Sino-Danish Center  
for Education and Research, Beijing 100190, China

<sup>\*\*\*</sup>Petrochina CoalBed Methane Company Limited, 100028, China

<sup>\*\*\*\*</sup>Yunnan Water Investment Company Limited, Kunming, 650106, China

(Received 27 July 2021 • Revised 17 November 2021 • Accepted 17 November 2021)

**Abstract**—Corn straw can be converted to bio-oil through pyrolysis. However, the application of bio-oil is severely restricted due to the high content of oxygen. Catalytic pyrolysis is an available way for deoxygenation of bio-oil, and the deoxygenation reactions are strongly dependent on the type of catalyst. Whereas, the correlation between the deoxygenated products and the catalyst types is still far from clear. In this work, the migration of O in the pyrolysis process was investigated, and eight catalysts were screened for deoxygenation of bio-oil, with a lab-scale fixed-bed reactor. The results showed that with the increase of pyrolysis temperature, the content of O in bio-oil decreased below 400 °C and then became stable and finally increased rapidly after 550 °C, indicating that the range of 400–550 °C was the proper temperature for deoxygenation. Eight catalysts (ZSM-5, SAPO-34, ZnO, MgO,  $\delta$ -Al<sub>2</sub>O<sub>3</sub>,  $\gamma$ -Al<sub>2</sub>O<sub>3</sub>, acidified- $\alpha$ -Al<sub>2</sub>O<sub>3</sub> and acidified- $\gamma$ -Al<sub>2</sub>O<sub>3</sub>) were tested, and it was found that a higher alkalinity of catalyst was favorable for decarboxylation of bio-oil with more produced CO<sub>2</sub>, while a higher acidity was promoted the decrease of alcohols and carbonyls with more generation of H<sub>2</sub>O and/or CO. MgO was judged as the optimal catalyst for deoxygenation of bio-oil. The quality of bio-oil under the catalysis of MgO was best, with higher H/C and lower O/C.

Keywords: Corn Straw, Pyrolysis, Deoxygenation, Bio-oil, Catalysis

### INTRODUCTION

Biomass, as a type of renewable resource, can be converted to bio-oil through pyrolysis, with a potential for replacing petroleum-based products. However, the high content of oxygen severely restricts the application of bio-oil [1]. Therefore, a bio-oil with lower content of oxygen is favorable, and the usage of catalysts in the pyrolysis process (catalytic pyrolysis) is a possible way for deoxygenation of bio-oil [1–18]. In the process of catalytic pyrolysis, the oxygen in volatile is expected to be reduced with catalyst, to induce the migration of oxygen into gas phase.

The catalysts for deoxygenation can be mainly divided into four categories: inorganic salts (KCl, K<sub>2</sub>CO<sub>3</sub>, Ca(OH)<sub>2</sub>) [3,4], metal oxides (Al<sub>2</sub>O<sub>3</sub>, MgO, ZnO, CaO) [5–9], molecular sieves (ZSM-5, SAPO-34) [10,11], and composite materials (HZSM-5/Al<sub>2</sub>O<sub>3</sub>, HZSM-5/Cu, Pt-Ni/ $\gamma$ -Al<sub>2</sub>O<sub>3</sub>) [12–15]. Catalysts can promote the scission of C–O bond, facilitating the transfer of oxygen into gas phase [16]. Although the catalytic deoxygenation of bio-oil has been broadly studied, it is still far from practical application, possibly due to the less satisfactory effect or extremely high cost of the catalysts. So, it

is still necessary for extensive and intensive investigations.

Deoxygenation mechanisms are very complex and different from different catalysts [9,17]. For instance, there are three major approaches to deoxygenation—decarboxylation, decarbonylation, and dehydration—with three corresponding products of CO<sub>2</sub>, CO, and H<sub>2</sub>O [9,17,18]. The deoxygenated products are expected to be CO<sub>2</sub>, rather than CO or H<sub>2</sub>O, because of the higher deoxygenation efficiency of CO<sub>2</sub> (two O atoms in CO<sub>2</sub>) than that of CO and H<sub>2</sub>O. Moreover, a higher deoxygenation efficiency is usually based on the sacrifice of the yield of bio-oil or the content of organics in bio-oil. However, the distribution of the removed O among the three deoxygenated products, as well as the compromise between the deoxygenation efficiency and the content of organics in bio-oil, has seldom been discussed [2].

In this work, the migration of O in the process for pyrolysis of corn straw, as a typical biomass resource, was investigated and eight catalysts were screened for deoxygenation of bio-oil, with a lab-scale fixed-bed reactor.

### EXPERIMENTAL

#### 1. Materials

The corn straw feedstock was crushed with a pulverizer (<200 mesh). The particles were dried at 105 °C for 4 h to remove the free

<sup>†</sup>To whom correspondence should be addressed.

E-mail: wangze@ipe.ac.cn

Copyright by The Korean Institute of Chemical Engineers.

**Table 1. Proximate and ultimate analyses of the corn straw**

Proximate analysis (wt%)				Ultimate analysis (wt% ad)				
$M_{ad}$	$V_{ad}$	$C_{ad}$	$A_{ad}$	C	H	N	S	O*
1.19	75.04	15.96	7.82	44.43	5.95	1.16	0.16	40.48

\*By difference

water. The proximate and ultimate analyses of the raw material are given in Table 1.

Eight materials (<200 mesh) were investigated for catalyst screen, including four types of alumina ( $\delta$ - $Al_2O_3$ ,  $\gamma$ - $Al_2O_3$ , acidified- $\alpha$ - $Al_2O_3$  and acidified- $\gamma$ - $Al_2O_3$ ), two zeolites (ZSM-5, SAPO-34), an alkaline material (MgO), and a material with both of acidity and alkalinity (ZnO). The performance of  $SiO_2$ , as an inert material, was also tested as background of physical influence of catalyst. All catalysts were calcined at 750 °C for 4h by 20 °C/min before testing. The materials were all purchased from Sinopharm.

## 2. Experimental Procedure

Corn straw was pyrolyzed with a fixed-bed reactor (See Fig. 1 for equipment diagram). In each run of experiment: carrier gas of  $N_2$  (50 mL/min) was introduced from top of the tubular reactor (inner diameter of 26 mm and length of 590 mm) to purge air; the tubular reactor was then heated to a setting temperature (300–700 °C) by 20 °C/min; after 20 minutes' stabilization of the oven temperature, the quartz basket containing 2.4 g corn straw with 1.0 g catalyst (catalyst powders were equally located in the top and bottom sides of the corn straw bed) was put into the tubular reactor; pyrolysis happened and the produced volatiles were transported to the condensation system (−10 °C) with  $N_2$ ; the condensed bio-oil was trapped in the glass bottles, and the non-condensable gas was col-

lected in a gasbag. The reaction lasted for 60 min, and then the tubular reactor was taken out of the fixed bed for fast cooling with the presence of  $N_2$ . After reaction, the char in the quartz basket and the bio-oil in glass bottles were weighed.

## 3. Product Analysis

The composition of the bio-oil and gas products was, respectively, analyzed by GC/MS (QP-2020, SHIMADZU) and GC (GC-2014, SHIMADZU). In the GC/MS system, a DB-FFAP column (30 m-0.25 mm-0.25  $\mu$ m) was used. The oven temperature program was set as follows: started at 40 °C holding for 5 min; then increased to 100 °C by 5 °C/min holding for 3 min; finally to 240 °C by 5 °C/min for 1min. The GC inlet temperature was set as 240 °C. The temperature of the transfer line between GC and MS was 240 °C; the ion source temperature was 200 °C with EI energy of 70 eV and m/e range of 15–500. The components were identified by searching in the library of NIST-2014.

The contents of C, H, O, N, S in corn straw and in pyrolysis products were characterized using an element analyzer (Elementar, Vario Macrocube). Thermogravimetric analysis (STA-449C, Netzsch Germany) of corn straw was in the temperature range of 30–1,050 °C.

## 4. Data Processing

The yields of gas, bio-oil and char were defined as the ratio of the mass of a product to the mass of corn straw (wt%):

$$Y_i = \frac{m_i}{m_{\text{corn straw}}} \cdot 100\% \quad (1)$$

where, i indicates the products of gas, bio-oil, and char;  $m_i$  is the mass of product i;  $m_{\text{corn straw}}$  is the mass of corn straw for pyrolysis.

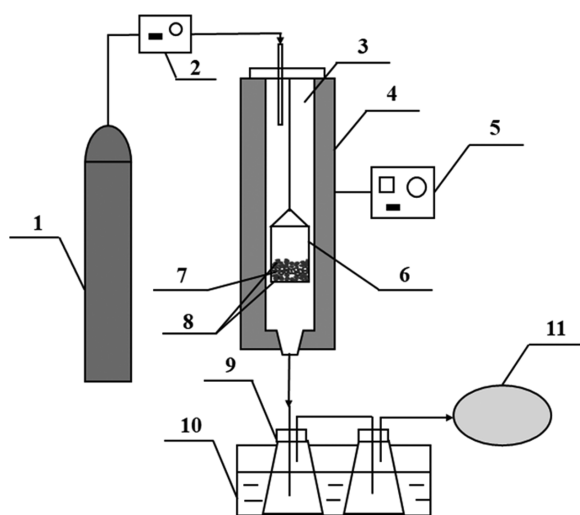
A special term, 'total deoxygenation', was defined as the summary mole of the removed O in the forms of  $CO_2$ , CO and  $H_2O$  in pyrolysis process, which could be expressed as the following equation:

$$T_{deOxy} = \sum_j O_j \cdot n_j \quad (2)$$

where, j indicates the products of  $CO_2$ , CO, and  $H_2O$ ;  $O_j$  is the number of O atom in the molecule of product j ( $O_{CO_2}=2$ ,  $O_{CO}=1$ ,  $O_{H_2O}=1$ );  $n_j$  is the mole of product j;  $T_{deOxy}$  is the sum of removed O atom (mol) in the three products of  $CO_2$ , CO,  $H_2O$ . The moles of  $CO_2$  and CO were obtained from GC analysis. The moles of  $H_2O$  were obtained by external-standard method, according to the peak area of water from analysis of GC/MS.

Taking the content of organics in the bio-oil without catalyst as standard, a special term of 'organics ratio' with the symbol of  $R_{RO}$  was defined, for indicating the ratio of organics in catalytic bio-oil to the non-catalytic case, which can be expressed as the following equation:

$$R_{RO} = \frac{m_{\text{Organics-cat}}/m_{\text{Bio-oil-cat}}}{m_{\text{Organics-non-cat}}/m_{\text{Bio-oil-non-cat}}} \cdot 100\% \quad (3)$$

**Fig. 1. Fixed-bed reactor for pyrolysis of corn straw.**

1.  $N_2$  cylinder
2. Mass flowmeter
3. Quartz tubular reactor
4. Tubular oven
5. Temperature controller
6. Quartz basket
7. Corn straw
8. Catalyst layer in both ends of corn straw
9. Glass bottles for liquid collection
10. Cooling pool
11. Gasbag

**Table 2. Specific surface area and average pore size of catalysts**

Catalyst	Specific surface area (m <sup>2</sup> /g)	Average pore diameter (nm)
$\delta$ -Al <sub>2</sub> O <sub>3</sub>	128.41	23.08
$\gamma$ -Al <sub>2</sub> O <sub>3</sub>	178.71	10.64
Acidified- $\alpha$ -Al <sub>2</sub> O <sub>3</sub>	147.05	6.41
Acidified- $\gamma$ -Al <sub>2</sub> O <sub>3</sub>	199.49	4.89
ZnO	2.78	13.59
MgO	26.59	55.16
SAPO-34	449.02	2.27
ZSM-5	316.93	2.48

$$m_{\text{organics}} = m_{\text{bio-oil}} - m_{\text{water}} \quad (4)$$

where,  $m_{\text{Bio-oil}_{\text{cat}}}$ ,  $m_{\text{Bio-oil}_{\text{non-cat}}}$ ,  $m_{\text{Organics}_{\text{cat}}}$  and  $m_{\text{Organics}_{\text{non-cat}}}$ , respectively, indicated the mass of bio-oil and the mass of organics in the bio-oil with and without catalyst;  $m_{\text{bio-oil}}$ ,  $m_{\text{water}}$  and  $m_{\text{organics}}$  are the mass of bio-oil, water in bio-oil, and organics in bio-oil, respectively.

The main deoxygenation products were CO<sub>2</sub>, CO and H<sub>2</sub>O. The distribution of the removed O atom in the three deoxygenated products of CO, CO<sub>2</sub>, H<sub>2</sub>O was discussed, with the following data processing methods:

$$R_j = \frac{n_j}{\sum_j n_j} \cdot 100\% \quad (5)$$

$R_j$  is the molar ratio of product  $j$  to the sum of the three products of CO<sub>2</sub>, CO, H<sub>2</sub>O.

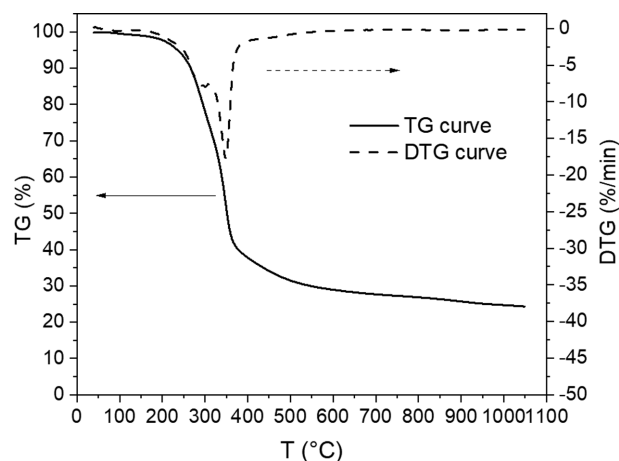
## 5. Catalyst Characterization

The texture properties of the catalysts were characterized by nitrogen adsorption method with a physical adsorption analyzer (Quantachrome, Autosorb-iQ-3). The samples were degassed at 150 °C for 6 h first, and then the adsorption of N<sub>2</sub> over the catalysts at 77 K was conducted. From the adsorption-desorption isotherms, the specific surface area and the average pore diameter of the samples were obtained. The data are listed in Table 2. It can be seen that the specific surface areas of the two zeolites of SAPO-34 and ZSM-5 are largest, while the areas of MgO and ZnO are smallest, and the areas of the four types of Al<sub>2</sub>O<sub>3</sub> ( $\delta$ -Al<sub>2</sub>O<sub>3</sub>,  $\gamma$ -Al<sub>2</sub>O<sub>3</sub>, acidified- $\alpha$ -Al<sub>2</sub>O<sub>3</sub>, acidified- $\gamma$ -Al<sub>2</sub>O<sub>3</sub>) are moderate. By contrast, the pore diameters of MgO and ZnO are largest, while the pores of zeolites are smallest, and the sizes of the four Al<sub>2</sub>O<sub>3</sub> catalysts are in the middle as well.

## RESULTS AND DISCUSSION

### 1. TG Analysis of Corn Straw

Thermogravimetric analysis of corn straw was conducted from 30 °C to 1,050 °C in N<sub>2</sub> atmosphere (50 ml/min), with a heating rate of 20 °C/min. The TG and DTG curves are shown in Fig. 2. It can be seen that several stages of weight loss appeared. The first stage (35–200 °C) can be attributed to the removal of crystal water. The second stage (200–450 °C) indicates the decomposition of organic matters in corn straw with a weight loss percentage of 65.6%. The third stage (450–700 °C) could correspond to deep cracking and

**Fig. 2. TG and DTG curves of the pyrolysis of corn straw from 30 °C to 1,050 °C.****Table 3. Yields of products varied with increasing temperature**

T (°C)	Yield (wt%)			
	Gas	Bio-oil	Char	Total
300	4.08	11.11	80.62	95.81
350	9.91	26.12	59.03	95.07
400	14.48	37.11	43.71	95.29
450	15.50	40.62	38.44	94.56
500	17.24	41.06	36.63	94.93
550	19.59	44.15	33.39	97.14
600	22.84	39.51	31.81	94.17
650	27.44	38.49	30.29	96.21
700	32.38	34.10	27.92	94.40

carbonization of organics in char. When the temperature was increased to over 700 °C, the inorganic matters in the residue began to decompose and/or sublimate.

### 2. Pyrolysis of Corn Straw without Catalyst

#### 2-1. Yields of Products

The pyrolysis of corn straw without catalyst was investigated using a fix-bed reactor. The yields of incondensable gas, bio-oil and char varied with increasing temperature in the range of 300–700 °C are shown in Table 3. The results show that the summary yields of the three phases of products were no less than 94%, indicating qualified reliability of data. With the increase of pyrolysis temperature, the yield of char decreased monotonically, while the yield of gas increased oppositely. The yield of bio-oil increased first and then decreased with increasing temperature, with a maximum value at 550 °C. The low yield of bio-oil at low temperature can be attributed to the low degree of pyrolysis. Whereas, under a high temperature over 550 °C, some components of bio-oil can be converted to gas products by deep-cracking, leading to the decrease of bio-oil.

#### 2-2. Composition of Gas Product

The influence of pyrolysis temperature on the composition of gas product is shown in Fig. 3. It can be seen that CO<sub>2</sub> and CO are two major gas components. With the increase of temperature, the

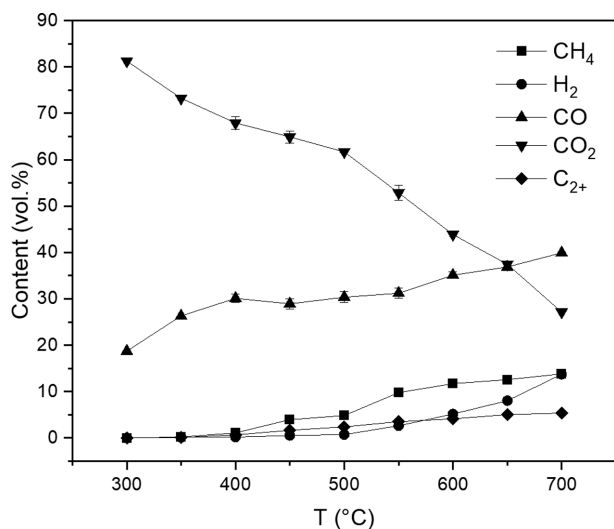


Fig. 3. Composition of gas product varied with increasing temperature.

content of CO<sub>2</sub> decreases continuously, while all other components including H<sub>2</sub>, CH<sub>4</sub> and small hydrocarbons (C<sub>2+</sub>) increase contrarily.

#### 2-3. Composition of Bio-oil

The contents of main groups of components and the contents of some typical organics in bio-oil varied with temperature are,

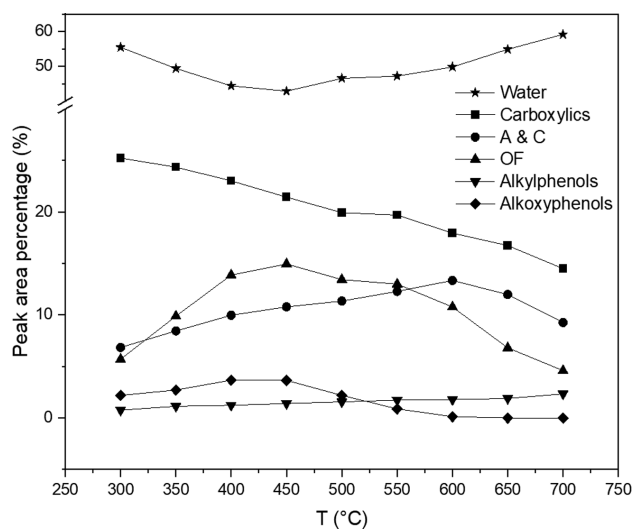


Fig. 4. Contents of main groups of organics in bio-oil varied with temperature (A&C- alcohols and carbonyls; OF- oxygen-containing compounds with a five-membered ring).

respectively, shown in Fig. 4 and Fig. 5. It can be seen that the content of water decreases with increasing temperature before 400 °C, and then becomes stable in the range of 400-550 °C, and finally increases with increasing temperature rapidly after 550 °C. The

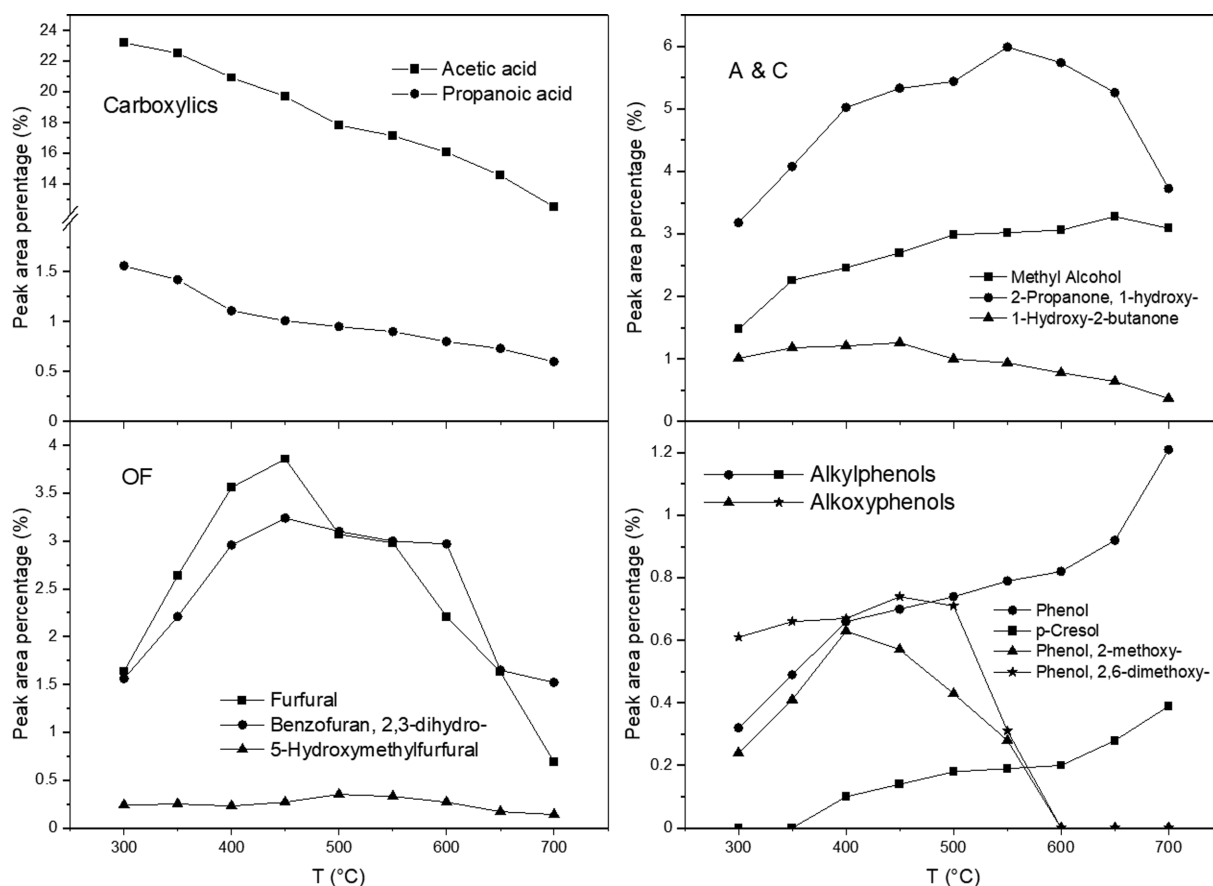


Fig. 5. Contents of typical organics in bio-oil varied with temperature.

composition of the organics is very complex, and mainly composed of carboxylics, alcohols and carbonyls (A&C), oxygen-containing compounds with a five-membered ring (OF), alkylphenols, and alkoxyphenols.

With the increase of temperature, the amount of carboxylics (like acetic acid and propanoic acid) in bio-oil decreases remarkably, while alkylphenols (like phenol and p-cresol) are more generated at high temperature. The alkoxyphenols (like creosol and 2,6-dimethoxy-phenol), the oxygen-containing compounds with a five-membered ring (like furfural, 5-hydroxymethylfurfural, and 2,3-dihydro-benzofuran), and the group of alcohols and carbonyls (like methanol, 1-hydroxy-2-butanone, 1-hydroxy-2-propanone) increase first and then decrease with increasing temperature. It indicates that the carboxylic compounds might convert to alcohols and carbonyls through decarboxylation with formation of  $\text{CO}_2$ . The oxygen-containing compounds with a five-membered ring derived from cellulose or hemi-cellulose can easily be produced at lower temperature, and may be further converted to other oxygenated products with the increase of temperature. Similarly, the lignin-derived alkoxyphenols from can be generated easier and then further converted to alkylphenols at higher temperature.

#### 2-4. Contents of C, H, O, N, S in Char

The influence of temperature on the contents of C, H, O, N, S in char is shown in Fig. 6. It can be seen that the char is rich in C and O. With the increase of temperature, the content of C increases rapidly before 400 °C and then turns to a mild increasing trend. The variation of O is just opposite to that of C, with a fast decreasing rate in early stage and a slow rate after 400 °C. The H in char decreases monotonically with increasing temperature. Both of N and S increase in early stage and then decrease.

#### 2-5. Contents of C, H, O, N, S in Bio-oil

The contents of C, H, O, N, S in bio-oil are shown in Fig. 7. It can be seen that the element of O is most abundant because of the high content of water in bio-oil. With the increase of temperature, the content of O decreases before 400 °C and then becomes stable and finally increases rapidly after 550 °C, which is just accordant

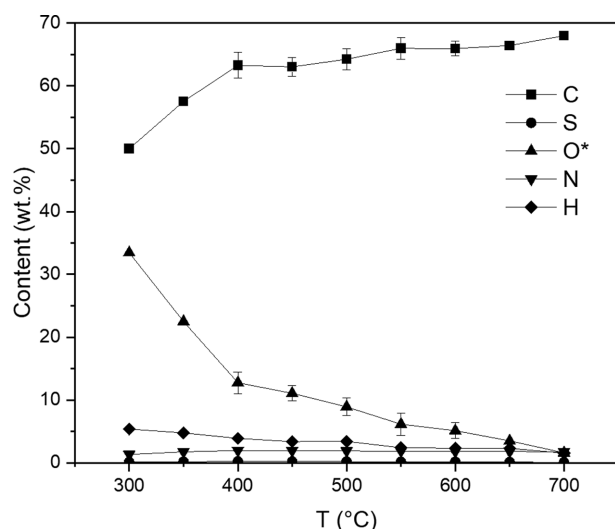


Fig. 6. Contents of C, H, O, N, S in char varied with temperature.

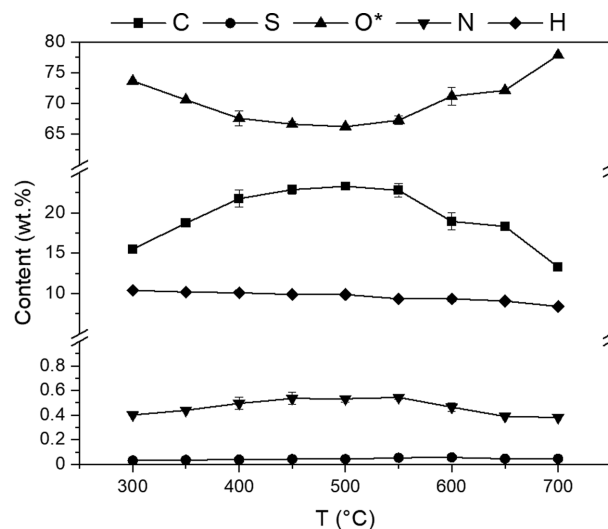


Fig. 7. Contents of C, H, O, N, S in bio-oil varied with temperature.

with the tendency of water content in bio-oil. The contents of C, N and S illustrate opposite trends to that of O. The H in bio-oil is generally stable and just slightly decreases with increasing temperature.

### 3. Pyrolysis of Corn Straw with Catalyst

As known from the above discussion, 400–550 °C is the proper range of temperature for pyrolysis of corn straw; a random value of 500 °C was selected as the temperature for the experiments with catalysts in the following section.

#### 3-1. Yields of Products

The yields of gas, bio-oil, and char from catalytic pyrolysis of corn straw at 500 °C are shown in Fig. 8. It can be seen that the yields of bio-oil are slightly reduced and meanwhile the gas products were more generated with all catalysts, compared with the non-catalytic or  $\text{SiO}_2$  system. Especially, the gas product is more produced under the roles of MgO and ZSM-5.

#### 3-2. Composition of Gas Product

The composition of the gas components from pyrolysis of corn

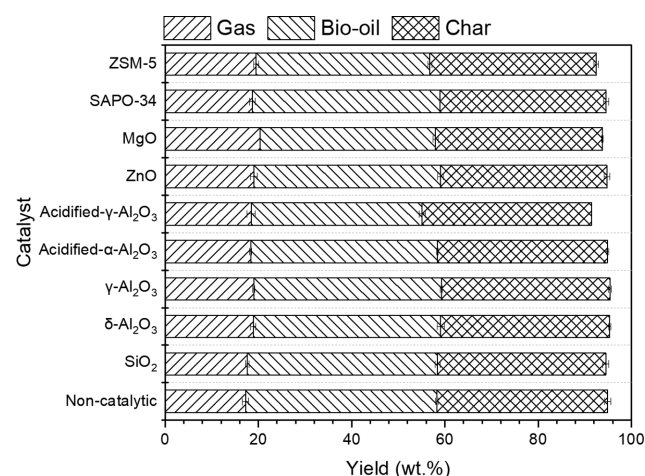


Fig. 8. Yields of gas, bio-oil, char from catalytic pyrolysis of corn straw at 500 °C.

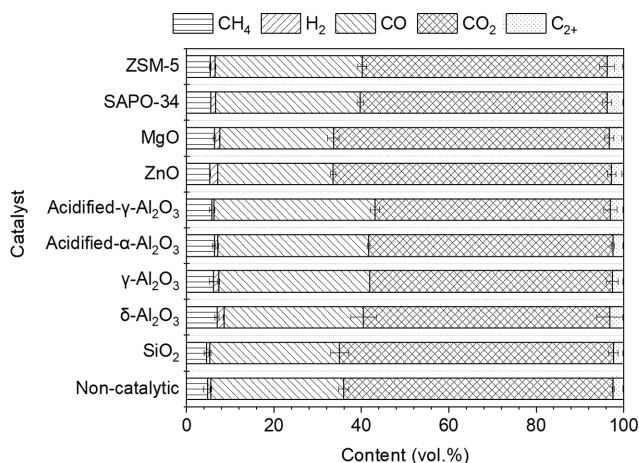


Fig. 9. Contents of gas components from catalytic pyrolysis of corn straw at 500 °C.

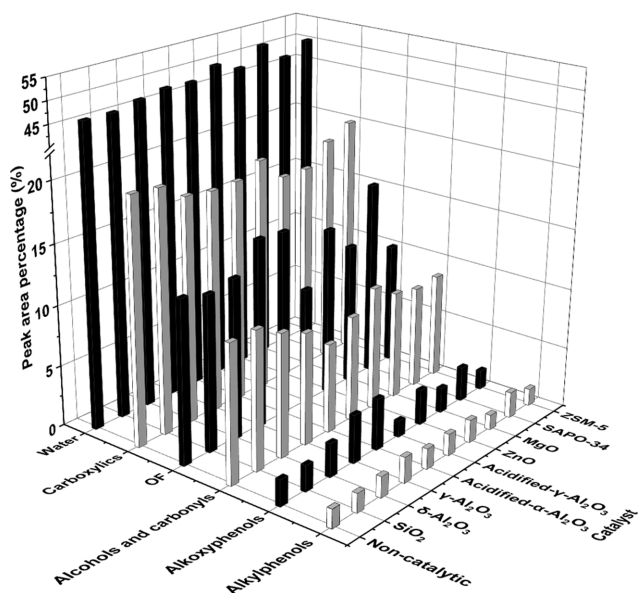


Fig. 10. Content of main components in bio-oil with different catalysts (A&C- alcohols and carbonyls; OF- oxygen-containing compounds with a five-membered ring).

straw with different catalysts at 500 °C is shown in Fig. 9. It can be seen that  $\text{CH}_4$  and the small hydrocarbons ( $\text{C}_{2+}$ ) are more generated in all catalytic systems. The formation of CO is promoted, while the generation of  $\text{CO}_2$  is inhibited, under the effects of  $\text{Al}_2\text{O}_3$  and zeolite types of catalysts. On the contrary, with the catalysts of MgO and ZnO,  $\text{CO}_2$  is more produced with less generation of CO, which is favorable for the improvement of deoxygenation efficiency.

### 3-3. Composition of Bio-oil

The contents of main groups of components in bio-oil with different catalysts are shown in Fig. 10. It can be seen that water is more generated with all catalysts, particularly under the roles of ZSM-5, MgO and acidified- $\gamma\text{-Al}_2\text{O}_3$ . The formation of the oxygen-containing compounds with a five-membered ring is promoted under the catalysis of  $\gamma\text{-Al}_2\text{O}_3$ , acidified- $\alpha\text{-Al}_2\text{O}_3$  and SAPO-34,

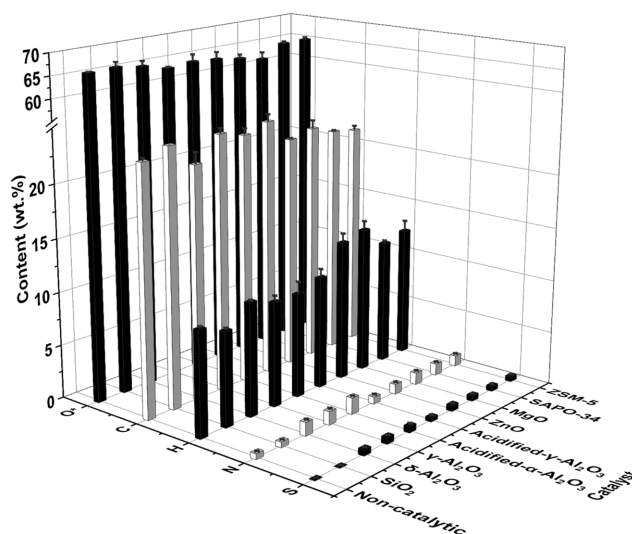


Fig. 11. Contents of C, H, O, S, N in bio-oil with different catalysts.

but severely inhibited with the role of acidified- $\gamma\text{-Al}_2\text{O}_3$  and ZSM-5. The contents of alcohols and carbonyls are generally reduced with all catalysts, which could correspond to the more water produced in bio-oil. The formation of alkoxyphenols was remarkably promoted with the catalysts of  $\gamma\text{-Al}_2\text{O}_3$  and acidified- $\alpha\text{-Al}_2\text{O}_3$ , while the contents of alkylphenols changed very little with most of the catalysts. The carboxylics were remarkably decreased with the catalysts of ZnO and MgO, which is accordant with more generated  $\text{CO}_2$  in gas product, indicating a higher deoxygenation efficiency of ZnO and MgO.

### 3-4. Contents of C, H, O, S, N in Bio-oil

The contents of C, H, O, S, N in bio-oil with different catalysts are characterized as shown in Fig. 11. It can be seen that the content of H in bio-oil increased remarkably with the catalysts of MgO, ZnO, ZSM-5 and SAPO-34, while the amount of O decreases more distinctly under the catalysis of MgO and ZnO. It indicates that the two materials of ZnO and MgO perform better than other catalysts, with a higher ratio of H/C in bio-oil. However, regrettably, the contents of S and N increase with all catalysts, which is disadvantageous for clean use of the bio-oil.

### 3-5. Distribution of the Removed O among $\text{CO}_2$ , CO and $\text{H}_2\text{O}$

The atomic efficiency of deoxygenation of the catalysts was evaluated through a comparison of the distributions of O among the three deoxygenated products of  $\text{CO}_2$ , CO and  $\text{H}_2\text{O}$ . A higher percentage of  $\text{CO}_2$  indicates a higher atomic efficiency of deoxygenation, since one C atom can take away two O atoms for  $\text{CO}_2$ . Whereas, only one O atom can be removed with one C atom or two H atoms for CO or  $\text{H}_2\text{O}$ . The normalized mole percentages of  $\text{CO}_2$ , CO and  $\text{H}_2\text{O}$  are shown in a ternary graph as shown in Fig. 12. It can be seen that under the catalysis of MgO, the fraction of  $\text{CO}_2$  is highest with less amount of  $\text{H}_2\text{O}$  and lower percentage of CO, indicating that the deoxygenation performance of MgO is best. The deoxygenation effect of ZnO is better too, with a higher fraction of  $\text{CO}_2$ , less  $\text{H}_2\text{O}$  and least CO. However, the performance of acidified- $\gamma\text{-Al}_2\text{O}_3$  is most undesirable, because the fraction of  $\text{CO}_2$  is lowest with the higher fractions of  $\text{H}_2\text{O}$  and CO.

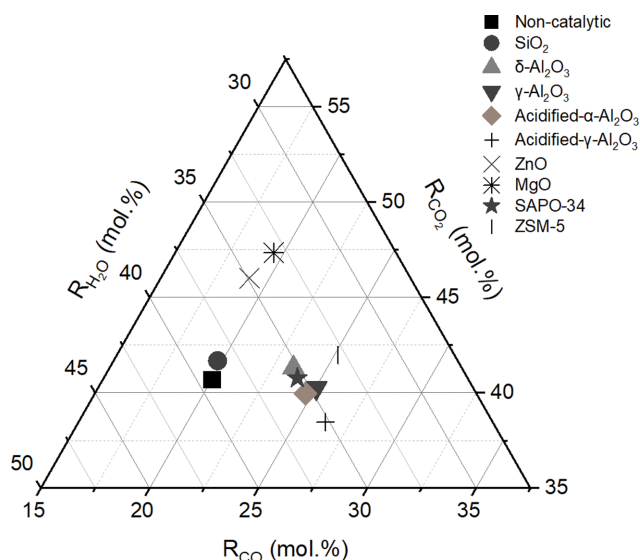


Fig. 12. Normalized mole percentages of the three deoxygenated products of CO<sub>2</sub>, CO and H<sub>2</sub>O with different catalysts.

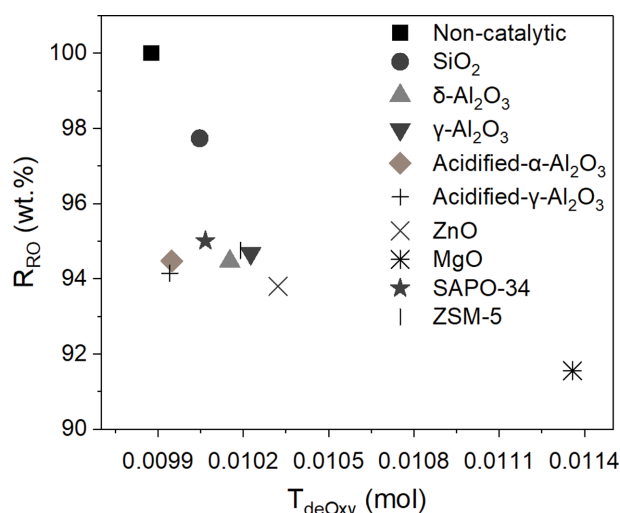


Fig. 13. Relationship between the total deoxygenation and the organics ratio of bio-oil with different catalysts.

### 3-6. Coordination of the Total Deoxygenation with the Organics Ratio

The amount of organics in bio-oil is usually in conflict with the amount of deoxygenation, so the compromise of the two factors with different catalysts is discussed herein. The coordination of the total deoxygenation with the organics ratio of bio-oil with different catalysts is shown in Fig. 13. It can be seen that the deoxygenation performance of MgO is highest, but with a low content of organics in bio-oil. Under the catalysis of ZnO, a higher content of organics in bio-oil can be achieved with a higher deoxygenation effect. In the two systems with acidified- $\alpha$ -Al<sub>2</sub>O<sub>3</sub> and acidified- $\gamma$ -Al<sub>2</sub>O<sub>3</sub>, the organics in bio-oil are more abundant, but the deoxygenation amounts are lowest.

### 3-7. Ratios of H/C and O/C in Bio-oil

The ratios of H/C and O/C in bio-oil with different catalysts are

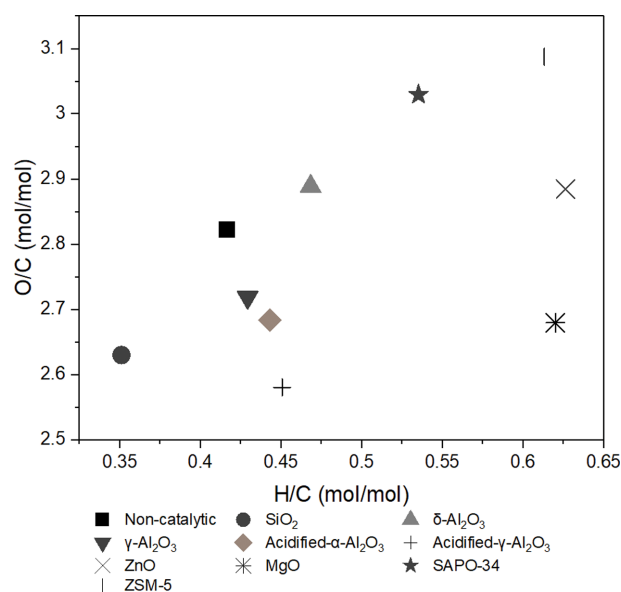


Fig. 14. Relationship between H/C and O/C of bio-oil with different catalysts.

shown in Fig. 14. It can be seen that the quality of the bio-oil from catalysis of MgO is best, with higher ratio of H/C and lowest ratio of O/C. The performance of ZnO is better too, with highest ratio of H/C but higher ratio of O/C either. For the bio-oil under catalysis of acidified- $\gamma$ -Al<sub>2</sub>O<sub>3</sub> or acidified- $\gamma$ -Al<sub>2</sub>O<sub>3</sub>, the ratio of O/C and the ratio of H/C are both lower. However, both of the ratios of H/C and O/C are higher, when catalyzed with ZSM-5 or SAPO-34. In general, from the viewpoint of bio-oil quality, the performance of MgO is best.

### 3-8. Mechanism Discussion

The specific surface areas of MgO and ZnO are much less than the areas of the two zeolites (SAPO-34 and ZSM-5) and those of the four Al<sub>2</sub>O<sub>3</sub> catalysts ( $\delta$ -Al<sub>2</sub>O<sub>3</sub>,  $\gamma$ -Al<sub>2</sub>O<sub>3</sub>, acidified- $\alpha$ -Al<sub>2</sub>O<sub>3</sub> and acidified- $\gamma$ -Al<sub>2</sub>O<sub>3</sub>), whereas the deoxygenation effects of MgO and ZnO are even higher with more generated CO<sub>2</sub>, which indicates that the texture properties of catalysts are not the critical factors for influencing the catalytic performance in this reaction system.

From the viewpoint of catalyst acidity, the eight catalytic materials can be divided into three classes: the acidic materials of  $\delta$ -Al<sub>2</sub>O<sub>3</sub>,  $\gamma$ -Al<sub>2</sub>O<sub>3</sub>, acidified- $\alpha$ -Al<sub>2</sub>O<sub>3</sub>, acidified- $\gamma$ -Al<sub>2</sub>O<sub>3</sub>, SAPO-34, and ZSM-5, the alkaline material of MgO, and the acid-base material of ZnO. Correlating the performance of the catalysts with the acidities of the catalysts, it can be deduced that a higher alkalinity is favorable for decarboxylation of bio-oil with more produced CO<sub>2</sub> (like ZnO or MgO), whereas a higher acidity of catalyst is promotive to the scissions of C-O, C-H and O-H bonds, leading to the decrease of alcohols and carbonyls with more generation of H<sub>2</sub>O and/or CO (like acidified- $\alpha$ -Al<sub>2</sub>O<sub>3</sub>, acidified- $\gamma$ -Al<sub>2</sub>O<sub>3</sub> and ZSM-5). Taking the role of ZnO with both of acidity and alkalinity for instance, according to the variations of organics, the mechanism for deoxygenation of carboxylics with ZnO can be deduced as Fig. 15 shows.

However, the role of catalysis is so complex that not all phenomena can be clearly correlated with the properties of different catalysts. There seems to be no definite regulations between the

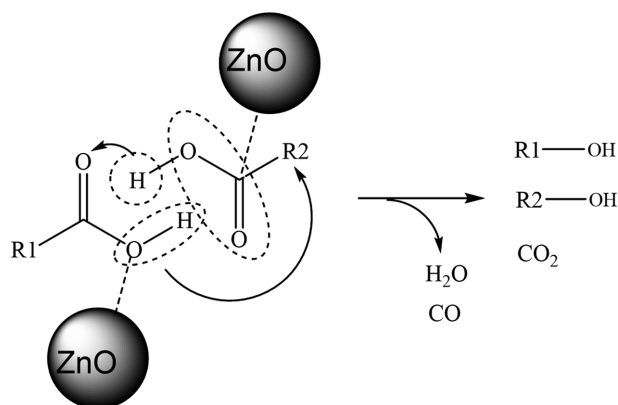


Fig. 15. Deduced mechanism for deoxygenation of carboxylics with catalysis of ZnO.

acidities of the catalysts and the variations of the alkoxyphenols or the oxygen-containing compounds with a five-membered ring. It indicates that the complicated catalytic effects may not only be related to the surface acidity, but also the surface charge, the pore size and the pore structure of materials, with complicated synergistic effects.

## CONCLUSION

To illustrate the influence of the catalyst type on the deoxygenation of bio-oil, the catalytic pyrolysis of corn straw was studied. The migration of O atom in the pyrolysis process was investigated, and eight catalysts were screened for deoxygenation of bio-oil with a lab-scale fixed-bed reactor. The results showed that with the increase of pyrolysis temperature, the content of O in bio-oil decreased below 400 °C and then became stable and finally increased rapidly after 550 °C, indicating that the range of 400–550 °C was the proper temperature for deoxygenation. Eight catalysts (ZSM-5, SAPO-34, ZnO, MgO,  $\delta$ -Al<sub>2</sub>O<sub>3</sub>,  $\gamma$ -Al<sub>2</sub>O<sub>3</sub>, acidified- $\alpha$ -Al<sub>2</sub>O<sub>3</sub> and acidified- $\gamma$ -Al<sub>2</sub>O<sub>3</sub>) were tested, and MgO was judged as the optimal catalyst for deoxygenation of bio-oil. With the catalysis of MgO or ZnO, the carboxylics in bio-oil decreased remarkably, which was accordant with the more generated CO<sub>2</sub> in gas product. Particularly, the quality of bio-oil under catalysis of MgO was best, with higher H/C and lower O/C. By contrast, the ratios of O/C and H/C were both lower with the catalyst of acidified- $\alpha$ -Al<sub>2</sub>O<sub>3</sub> or acidified- $\gamma$ -Al<sub>2</sub>O<sub>3</sub>, and both higher when catalyzed with ZSM-5 or SAPO-34. In general, a higher alkalinity of catalyst was favorable for decarboxylation of bio-oil, while a higher acidity promoted the decrease of alcohols and carbonyls with generation of more H<sub>2</sub>O and/or CO.

## ACKNOWLEDGEMENTS

We acknowledge financial support by the National Key R&D Program of China (2019YFC1906700).

## REFERENCES

1. H. Lee, Y.M. Kim and I. G. Lee, *Korean J. Chem. Eng.*, **33**, 3299 (2016).
2. X. Chen, Y. Chen, H. Yang, X. Wang, Q. Che, W. Chen and H. Chen, *Bioresour. Technol.*, **273**, 153 (2019).
3. X. Tian, Y. Wang, Z. Zeng, L. Dai, Y. Peng, L. Jiang, X. Yang, L. Yue, Y. Liu and R. Ruan, *Bioresour. Technol.*, **320**, 124415 (2021).
4. C. Wang, L. Li, Z. Zeng, X. Xu, X. Ma, R. Chen and C. Su, *Biore-sour. Technol.*, **281**, 412 (2019).
5. A. Eschenbacher, A. Saraeian, P.A. Jensen, B. H. Shanks, C. Li, J. Ø. Duus, T.E. L. Smitshuysen, C. D. Damsgaard, A. B. Hansen, K. I. Kling, U. V. Mentzel, U. B. Henriksen, J. Ahrenfeldt and A. D. Jensen, *Chem. Eng. J.*, **394**, 124878 (2020).
6. J. L. F. Oliveira, L. M. Batista, N. A. dos Santos, A. M. Araújo, V. J. Fernandes Jr., A. S. Araujo, A. P. Alves and A. D. Gondim, *Renew. Energy*, **168**, 1377 (2021).
7. Y. Lin, C. Zhang, M. Zhang and J. Zhang, *Energy Fuels*, **24**(10), 5686 (2010).
8. L. Santamaria, M. Artetxe, G. Lopez, M. Cortazar, M. Amutio, J. Bilbao and M. Olazar, *Fuel. Process. Technol.*, **198**, 106223 (2020).
9. A. N. K. Lup, F. Abnisa, W. M. A. W. Daud and M. K. Aroua, *Appl. Catal. A. Gen.*, **541**, 87 (2017).
10. A. Veses, B. Puértolas, J. M. López, M. S. Callén, B. Solsona and T. García, *ACS Sustain. Chem. Eng.*, **4**(3), 1653 (2016).
11. S. N. Liu, J. P. Cao, X. Y. Zhao, J. X. Wang, X. Y. Ren, Z. S. Yuan, Z. X. Guo, W. Z. Shen, J. Bai and X. Y. Wei, *J. Energy Inst.*, **92**(5), 1567 (2019).
12. A. Eschenbacher, P. A. Jensen, U. B. Henriksen, J. Ahrenfeldt, C. Li, J. Ø. Duus, U. V. Mentzel and A. D. Jensen, *Energy Fuels*, **33**(7), 6405 (2019).
13. N. Chaihad, A. Anniwaer, S. Karnjanakom, Y. Kasai, S. Kongpara-kul, C. Samart, P. Reubroycharoen, A. Abudula and G. Guan, *J. Anal. Appl. Pyrolysis*, **155**, 105079 (2021).
14. B. Puertolas, T. C. Keller, S. Mitchell and J. Pérez-Ramírez, *Appl. Catal. B*, **184**, 77 (2016).
15. H. Wang, W. Tian, F. Zeng, H. Du, J. Zhang and X. Li, *Fuel*, **282**, 118807 (2020).
16. Y. M. Kim, H. W. Lee, S. H. Jang, J. Jeong, S. Ryu, S. C. Jung and Y. K. Park, *Korean J. Chem. Eng.*, **37**(3), 493 (2020).
17. Q. Zhou, A. Zarei, A. De Girolamo, Y. Yan and L. Zhang, *J. Anal. Appl. Pyrolysis*, **139**, 167 (2019).
18. Y. Qian, J. Zhang and J. Wang, *Bioresour. Technol.*, **174**, 95 (2014).